

Empirical tight-binding model for the electronic structure of dilute GaNAs alloys

N. Shtinkov,* P. Desjardins, and R. A. Masut

*Département de Génie Physique and Groupe de Recherche en Physique et Technologie des Couches Minces (GCM),
École Polytechnique de Montréal, C.P. 6079, Succursale "Centre-Ville," Montréal QC, Canada H3C 3A7*

(Received 28 November 2002; published 28 February 2003)

We present an empirical tight-binding (TB) model for the electronic structure of $\text{GaN}_x\text{As}_{1-x}$ with nitrogen content $x < 5\%$, over the entire Brillouin zone. The model upgrades existing TB schemes, introducing an additional s orbital to account for the N-induced change of conduction-band states. The resulting band structure is analyzed using an $sp^3d^5s^*$ TB parametrization and compared to experimental and other theoretical data. The model reproduces the results of the band anticrossing model at the Γ point of the Brillouin zone, and the dependence of the X and L band-edge states on the N concentration is in good agreement with experimental data. The model is readily applicable to electronic structure calculations of other III-N-V compounds and heterostructures.

DOI: 10.1103/PhysRevB.67.081202

PACS number(s): 71.15.Ap, 71.20.Nr

Semiconductor III-N-V alloys, in which the group-V element is partially replaced by nitrogen, have been a subject of extensive investigation in recent years due to their unusual properties. The addition of only 1% of nitrogen in GaAs leads to a band-gap reduction of almost 0.2 eV,¹ opening a wide range of potential applications for long-wavelength optoelectronic devices. A simple, reliable model for calculating the electronic structure of these materials is needed for interpretation of experimental data, as well as for predicting and optimizing heterostructure device properties.

Various theoretical methods have been used in order to understand the electronic structure of $\text{GaN}_x\text{As}_{1-x}$. First-principles,² empirical pseudopotential,³ and sp^3s^* tight-binding⁴ (TB) calculations of large supercells have been performed, providing valuable insight into the microscopic mechanisms of formation of band-edge states in $\text{GaN}_x\text{As}_{1-x}$. However, these supercell calculations are not suitable for heterostructure modeling because of their computational complexity.

In the band anticrossing (BAC) model,⁵ the electronic structure of $\text{GaN}_x\text{As}_{1-x}$ is calculated based on the assumption that the conduction-band states of the alloy are formed due to an anticrossing interaction between the extended states of the GaAs bulk band edge and a higher-lying band of localized states of the substitutional N atoms.⁶ The two-level Hamiltonian of the system is⁵

$$H_{\text{BAC}} = \begin{pmatrix} E_C & V_{\text{CN}} \\ V_{\text{CN}} & E_N \end{pmatrix}, \quad (1)$$

where $E_C = E_C^0 + \hbar^2 k^2 / 2m^*$ is the energy of the unperturbed GaAs conduction band, E_N is the N impurity state energy, and the interaction matrix element depends on the nitrogen fraction x as $V_{\text{CN}} = x^{1/2} C_N$, where C_N is an empirical constant. Besides the original two-level BAC model,⁵ the same idea can be incorporated into a $\mathbf{k} \cdot \mathbf{p}$ scheme.⁷⁻⁹ This approach yields an excellent quantitative description of the Γ conduction-band states of $\text{GaN}_x\text{As}_{1-x}$: compositional dependence of the lowest experimentally observed transitions (usually labeled E_- and E_+), increase of the electron effective mass, and anomalous pressure dependence of the energy

band gap. Its simplicity and accuracy have made it the preferred tool for calculating the electronic structure of dilute nitride alloys and heterostructures.

The BAC model and similar $\mathbf{k} \cdot \mathbf{p}$ models are intrinsically limited to the vicinity of the Γ point of the Brillouin zone (BZ). An attempt to extend the BAC model to the whole BZ has been made,⁹ but it requires the band dispersion of the host material as an input parameter. There is already a significant accumulation of experimental data on electronic transitions at the X and L points of the BZ. Experimental observations of the E_1 transition (originating from the L point of the BZ) indicate that it also depends on the N concentration, although this dependence is weaker than for the E_+ and E_- transitions.¹⁰⁻¹⁶ On the other hand, the E_2 transition (originating from states around the X point) is virtually independent of the N fraction.^{11,12,15} The recent observation of a new transition, labeled E^* ,^{13,14} suggests that the L conduction-band states exhibit behavior similar to that of the E_+ and E_- transitions at Γ . So far, these results have not received a consistent interpretation within a single band-structure model.

In the present work we develop an alternative approach to the calculation of the electronic structure of $\text{GaN}_x\text{As}_{1-x}$ within the semiempirical tight-binding framework. The proposed model conserves the crystal periodicity; therefore, its computational complexity is comparable to that of the BAC model. The properties of the model are discussed and the band structure of $\text{GaN}_x\text{As}_{1-x}$ for $0 < x < 5\%$ is calculated using an $sp^3d^5s^*$ TB parametrization. The behavior of the band-edge states at Γ , X , and L is analyzed and it is shown that the predictions of our model agree very well with experimental observations.

The majority of the experimental results on $\text{GaN}_x\text{As}_{1-x}$ show that the major changes in the band structure due to the incorporation of nitrogen occur in the vicinity of the conduction-band minimum.¹⁰⁻¹⁶ The change of the higher-energy conduction bands can usually be described in terms of relatively small bowing parameters, while modifications of the valence bands are considered negligible. This observation makes possible the BAC description of the electronic structure, where the effect of substitutional nitrogen is ac-

counted for by introducing a dispersionless impurity band with energy above the conduction-band minimum. In our TB description we follow the same approach, aimed at obtaining a TB Hamiltonian that reproduces the anticrossing behavior of the conduction-band states and leaves unmodified the valence-band structure. We use the virtual crystal approximation and describe the bulk bands in terms of a basis set of Bloch functions. Instead of fitting an entire parameter set in order to reproduce the $\text{GaN}_x\text{As}_{1-x}$ band structure, we “upgrade” existing TB schemes, adding to the GaAs basis set an additional anion s orbital, s_N , to account for the spherically symmetrical states of substitutional nitrogen atoms. To introduce repulsive interaction between the N subband and the host conduction band (constructed predominantly by s orbitals), we let the s_N orbital couple with the nearest-neighbor (cation) s orbitals. All the matrix elements between s_N and the other orbitals are set to zero in order to minimize the effect of the s_N orbital on the valence bands and on the conduction bands at X . Thus, we introduce only two additional parameters: the on-site energy for the s_N orbital, E_s^N , and the two-center integral $s_c s_N \sigma$.

These two parameters are related to the two parameters of the BAC model, C_N and E_N . Using the expansion of the wave function of the GaAs conduction-band edge

$$\psi_{CB}(\text{GaAs}) = \sum_{\alpha,j} A_{\alpha}^j |\alpha_j\rangle, \quad (2)$$

where $j=c,a$ stands for cation/anion, $\alpha=s,p,d,\dots$ are the basis orbitals, and A_{α}^j are the expansion coefficients, one may express E_N and V_{CN} in Eq. (1) in terms of TB matrix elements. This leads to the following relations between the TB and the BAC parameters:

$$E_s^N = E_N, \quad (3)$$

$$s_c s_N \sigma = -C_N x^{1/2} / 4 |A_s^c|, \quad (4)$$

where A_s^c is the coefficient before the $|s_c\rangle$ orbital in the normalized wave function of the GaAs conduction-band edge at Γ .

This procedure for constructing the new Hamiltonian by “upgrading” the GaAs TB Hamiltonian with a new orbital has several major advantages. First, we use the existing parameter sets reproducing the bulk band structure and introduce only two new parameters describing the effect of N, therefore it can be readily adapted for other III-N-V alloys exhibiting similar behavior. The new parameters are related to those used in the BAC model and in the cases where a BAC description is already available no additional fitting is needed. Finally, one is not limited to the use of a particular TB model (as is the case when fitting entire TB parameter sets), since the above procedure can be applied to all common TB parametrizations in a straightforward way.

The accuracy of the numerical results depends on that of the employed TB scheme. In our calculations we use the $sp^3d^5s^*$ TB model of Jancu *et al.*,¹⁷ which describes accurately the band dispersions of the III-V semiconductors for energies up to 6 eV above the valence-band maximum and

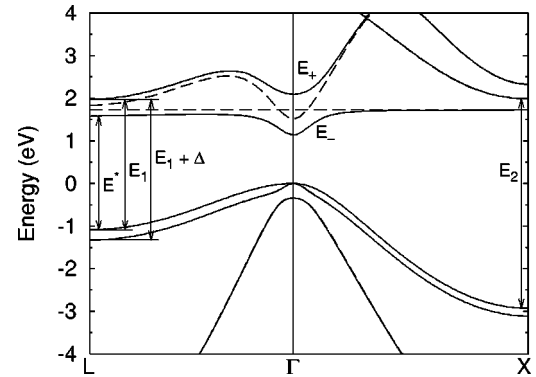


FIG. 1. Band structure of $\text{GaN}_x\text{As}_{1-x}$, calculated with the $sp^3d^5s^*s_N$ model for $x=0.03$ (solid line) and in the impurity limit $x \rightarrow 0$ (dashed line).

reproduces correctly the orbital character of the Γ , X , and L band-edge states and their behavior under strain.¹⁷ For pure GaAs, this model gives a direct gap of 1.519 eV and an electron effective mass of $0.067m_0$. For the energy of the N level we take the BAC value for zero temperature $E_N = 1.725$ eV, and for the coupling constant $C_N = 2.7$ eV.¹⁸ From Eq. (4) we obtain $s_c s_N \sigma = -1.000\sqrt{x}$ eV. The new $sp^3d^5s^*s_N$ basis consists of 42 orbitals: the original 40 plus two spin-degenerate s_N orbitals. The calculated band structure along the $\langle 111 \rangle$ and $\langle 100 \rangle$ directions is shown in Fig. 1 for $x=0$ (GaAs) and $x=0.03$. Due to the absence of s_N - p coupling, the valence-band structure remains independent of x . We observe two $\text{GaN}_x\text{As}_{1-x}$ conduction bands resulting from the anticrossing interaction of the GaAs lowest conduction band and the s_N band. We use the widely accepted BAC notation, E_- and E_+ , for the two conduction bands. Unlike the BAC results, however, the TB bands are valid over the entire BZ.

In the vicinity of Γ the behavior of the E_- and E_+ bands is similar to the results of the BAC model. There is, however, one significant difference: while in the BAC model the coupling matrix element V_{CN} is independent of the wave vector, its TB equivalent decreases away from the zone center because of the decreasing contribution of the s_c orbital to the GaAs conduction band. Thus, although the two models give identical results for the conduction-band states at Γ , the band dispersion is different, resulting in smaller electron effective mass in the TB model (Fig. 2). As seen from Fig. 2, our model predicts a decrease of m_e^* for $x > 1.5\%$. The theoretical effective masses in both TB and BAC models are

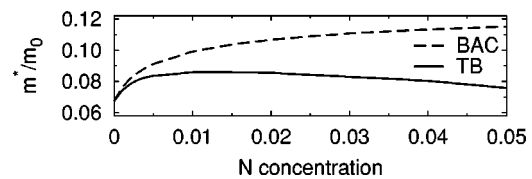


FIG. 2. Dependence of the electron effective mass on the N concentration x in $\text{GaN}_x\text{As}_{1-x}$, calculated with the TB model (solid line) and the BAC model (dashed line).

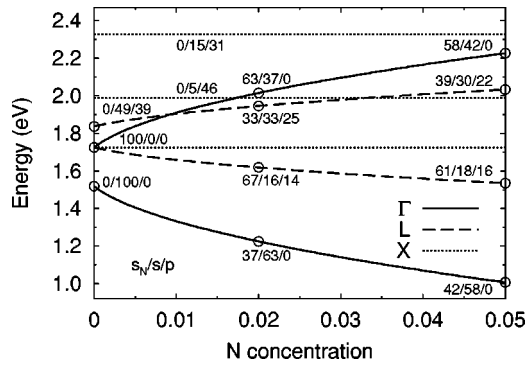


FIG. 3. Energies of the lowest Γ , X , and L states in the conduction band in $\text{GaN}_x\text{As}_{1-x}$ alloys. The numbers show the percentage contributions of s_N , other s ($s + s^*$), and p ($p_x + p_y + p_z$) orbitals to the wave functions of the states for 0, 2%, and 5% nitrogen content (shown with circles).

smaller than the reported experimental results for the electron effective mass in $\text{GaN}_x\text{As}_{1-x}$, which for $0.01 < x < 0.035$ are in the range $0.12 - 0.55m_0$.^{1,19,20} It is possible to alter the TB parameters in order to obtain greater values for m_e^* . However, given the scatter in the experimental data obtained by different authors and the uncertainties associated with these measurements, we prefer to preserve the simplicity and the convenience of the present TB scheme at least until definitive experimental results for the x dependence of the electron effective mass in $\text{GaN}_x\text{As}_{1-x}$ are available.

The calculated dependencies of the lowest Γ , X , and L conduction-band states on the N concentration are plotted in Fig. 3. The states $E_-(\Gamma)$ and $E_+(\Gamma)$ reproduce the results of the BAC model within 7 meV for x up to 5% (the latter are not shown in the figure, since they essentially coincide with the TB curves). The GaAs conduction-band minimum is composed entirely of s orbitals. The coupling between the two bands increases with x , which is reflected in the change of their orbital character—adding only 2% nitrogen increases the s_N contribution to the conduction-band minimum $E_-(\Gamma)$ from 0 to 37%. At X , the E_- and E_+ bands are completely uncoupled due to the vanishing of the s - s matrix element. Consecutively, their energies and orbital character remain independent of the N incorporation. At L the behavior is similar to that observed at Γ , however, the dependence on x is weaker due to the smaller s contribution to the L states (49% for pure GaAs versus 100% at Γ). Note that the lower-energy band E_- is of predominantly s character at Γ , and changes to mostly s_N at L . This is due to the band anticrossing in the $\langle 111 \rangle$ direction (see Fig. 1).

The obtained splitting of the L states and their dependence on the N concentration confirms the tentative explanation of the experimentally observed E^* transition¹³ as originating from a nitrogen-induced state at the L point of the conduction band. In order to compare our TB results with experimental data, we have compiled in Table I the measured dependencies of the E^* , E_1 , $E_1 + \Delta$, and E_2 transitions on the N concentration from several sources. In most experimental works the data are interpreted in terms of band bowing parameters and fitted with quadratic functions. We have used

TABLE I. Experimental and calculated (TB) slope (dE/dx) in eV of the dependencies of several transition energies on the N concentration x in $\text{GaN}_x\text{As}_{1-x}$.

Source	(E^*)	(E_1)	$(E_1 + \Delta)$	(E_2)
Reference 10		1.9	4.3	
Reference 11		2.664		
Reference 12		2.008	2.904	0.513
Reference 13	≈ -4.8	≈ 2.6		
Reference 14		2.9	2.8	
Reference 15		1.52	4.046	-1.008
Reference 16		2.53		-1.69
TB	-6.0	3.233	4.167	-0.467

linear approximations instead, since the quadratic terms are negligible in the considered range of N concentrations. The TB results in the table are obtained using a linear approximation between the calculated transition energies for pure GaAs and at $x=0.03$. The $\text{GaN}_x\text{As}_{1-x}$ alloys are considered coherently grown on a GaAs (001) substrate, resulting in a biaxial tensile strain. The strain is taken into account by scaling the two-center integrals ijk with the bond length

$$ijk(d) = \left(\frac{d}{d_0}\right)^{\nu_{ijk}} ijk(d_0), \quad (5)$$

where $d(d_0)$ is the strained (unstrained) interatomic distance. The bond angle changes are accounted for within the virtual crystal approximation. For the exponents ν_{ijk} we use the values of Ref. 17, which are obtained by fitting the bulk deformation potentials. The strain-induced splitting of the on-site d -orbital energies is also taken into account.¹⁷ The two-center integral $s_N s_c \sigma$ is considered independent of strain, since taking $\nu_{s_N s_c \sigma} = 4$ in Eq. (5) changes the energies of the conduction-band states by less than 1 meV per 1-at. % nitrogen. The lattice constant and the elasticity moduli of $\text{GaN}_x\text{As}_{1-x}$ are calculated from a linear approximation between GaAs and cubic GaN, using the values from Ref. 21. The transition energies are calculated at the L point of the BZ for E^* , E_1 , and $E_1 + \Delta$ and at the X point for the E_2 transition, as shown in Fig. 1. Note that at X the transition probability between the valence bands and the E_- band is zero, since the latter has entirely s_N character. Therefore, the lowest-energy optical transition at X is between E_+ and the valence band. The TB value for the slope of the E_2 transition is an average between the calculated values for the in-plane and perpendicular X points (-0.867 eV and -0.067 eV, respectively), which are nonequivalent due to strain.

It is seen from Table I that the calculated variations of the transition energies are in good agreement with the experimental results. The calculated slopes for $E_1 + \Delta$ and E_2 fall within the range of the experimentally measured values. For all the transitions except E_1 the difference between the calculated and the measured slope dE/dx is less than 1.4 eV (i.e., 14 meV%), which is quite reasonable given the scatter in the experimental results obtained by different authors. For the E_1 transition, all the measured dependencies of the en-

ergy on x have smaller slopes than our calculated value of 3.233 eV, the maximum difference being again relatively small (1.713 eV). A possible explanation of this observation is the fact that states from other points in the BZ along the $\langle 111 \rangle$ direction also contribute to E_1 , and their dependence on x is somewhat weaker than that of the L -point states. On the other hand, not taking into account the E^* and the $E^* + \Delta$ transitions, which are close in energy to E_1 and have the opposite dependence on x , can effectively lower the experimentally measured slope of E_1 .

The accuracy of our results for the L - and X -point transitions is plausible, given that we used only the BAC parameters fitted for Γ in order to describe the band anticrossing effects in the entire BZ. This gives another confirmation of the assumption that the conduction-band formation in $\text{GaN}_x\text{As}_{1-x}$ is driven by the anticrossing interaction between the host bands and the localized N states throughout the entire BZ. One must keep in mind, however, that the broken crystal periodicity in the alloy may lead to coupling of host states from different \mathbf{k} points in the BZ,²⁻⁴ which cannot be reproduced by our model. The TB scheme proposed in the present work is essentially band anticrossing in nature, and as such, it does not account for the effects of the alloy fluctuations, disorder, clustering, and local lattice distortions due to the incorporation of N atoms. Nevertheless, our calculations yield excellent results for the energies of the electronic states at least at the Γ , X , and L points of the BZ.

While retaining the accuracy of the BAC results at Γ , the proposed TB model has significant advantages compared

with the original two-level BAC model and derived $\mathbf{k}\cdot\mathbf{p}$ schemes. It presents a unified band anticrossing picture of the $\text{GaN}_x\text{As}_{1-x}$ electronic structure over the entire BZ for a wide energy range, using the same number of adjustable parameters as the BAC model. The use of the virtual crystal approximation, while neglecting effects such as mixing of states from different points in the BZ, retains the simplicity and the flexibility characteristic for TB models, allowing for easy calculation of heterostructures and straightforward incorporation of the effects of strain, pressure, and applied electric field.

In summary, we have developed an empirical tight-binding method for calculating the electronic structure of $\text{GaN}_x\text{As}_{1-x}$ alloys over the entire BZ, upgrading existing TB models by an additional anion s orbital in order to account for the N-induced change of the conduction-band states. Two new parameters are introduced, which are related to the parameters of the BAC model, making our approach easily transferable to various TB parametrizations and to other III-V compounds. Our results for the transition energies at Γ , L , and X agree with experimental data. The simplicity and flexibility of the proposed approach make it easily usable in band-structure calculations of III-N-V alloys and heterostructures.

We thank the authors of Ref. 15 for providing their manuscript prior to publication. This work was financially supported by the Natural Sciences and Engineering Research Council of Canada. P.D. also acknowledges support from the Canada Research Chair Program.

*Electronic address: nshtinkov@polymtl.ca

¹I.A. Buyanova, W.M. Chen, and B. Monemar, MRS Internet J. Nitride Semicond. Res. **6**, 2 (2002).

²L.-W. Wang, Appl. Phys. Lett. **78**, 1565 (2001); B.K. Agrawal, P.S. Yadav, R. Srivastava, and S. Agrawal, J. Phys.: Condens. Matter **10**, 4597 (1998).

³T. Mattila, S.-H. Wei, and A. Zunger, Phys. Rev. B **60**, R11 245 (1999); P.R.C. Kent and A. Zunger, *ibid.* **64**, 115208 (2001).

⁴A. Lindsay and E.P. O'Reilly, Solid State Commun. **112**, 443 (1999); **118**, 313 (2001).

⁵W. Shan, W. Walukiewicz, J.W. Ager III, E.E. Haller, J.F. Geisz, D.J. Friedman, J.M. Olson, and S.R. Kurtz, Phys. Rev. Lett. **82**, 1221 (1999).

⁶J. Wu, W. Shan, and W. Walukiewicz, Semicond. Sci. Technol. **17**, 860 (2002).

⁷E.P. O'Reilly and A. Lindsay, Phys. Status Solidi B **216**, 131 (1999).

⁸P.J. Klar, H. Grüning, W. Heimbrod, J. Koch, W. Stolz, P.M.A. Vicente, A.M. Kamal Saadi, A. Lindsay, and E.P. O'Reilly, Phys. Status Solidi B **223**, 163 (2001).

⁹E.P. O'Reilly, A. Lindsay, S. Tomić, and M. Kamal-Saadi, Semicond. Sci. Technol. **17**, 870 (2002).

¹⁰G. Leibiger, V. Gottschalch, B. Rheinländer, J. Šik, and M. Schubert, Appl. Phys. Lett. **77**, 1650 (2000).

¹¹W. Shan, W. Walukiewicz, K.M. Yu, J.W. Ager, E.E. Haller, J.F. Geisz, D.J. Friedman, J.M. Olson, S.R. Kurtz, and C. Nauka, Phys. Rev. B **62**, 4211 (2000).

¹²W.K. Hung, M.Y. Chern, Y.F. Chen, Z.L. Yang, and Y.S. Huang, Phys. Rev. B **62**, 13 028 (2000).

¹³J.D. Perkins, A. Mascarenhas, J.F. Geisz, and D.J. Friedman, Phys. Rev. B **64**, 121301 (2001).

¹⁴U. Tisch, E. Finkman, and J. Salzman, Phys. Rev. B **65**, 153204 (2002).

¹⁵G. Leibiger, V. Gottschalch, V. Riede, M. Schubert, J. N. Hilfiker, and T. E. Tiwald (unpublished).

¹⁶S. Matsumoto, H. Yaguchi, S. Kashiwase, T. Hashimoto, S. Yoshida, D. Aoki, and K. Onabe, J. Cryst. Growth **221**, 481 (2000).

¹⁷J.-M. Jancu, R. Scholz, F. Beltram, and F. Bassani, Phys. Rev. B **57**, 6493 (1998).

¹⁸C. Skierbiszewski, Semicond. Sci. Technol. **17**, 803 (2002).

¹⁹Y. Zhang, A. Mascarenhas, H.P. Xin, and C.W. Tu, Phys. Rev. B **61**, 7479 (2000).

²⁰P.N. Hai, W.M. Chen, I.A. Buyanova, H.P. Xin, and C.W. Tu, Appl. Phys. Lett. **77**, 1843 (2000).

²¹I. Vurgaftman, J.R. Meyer, and L.R. Ram-Mohan, J. Appl. Phys. **89**, 5815 (2001).